

2

Memantine as an Example of a Fast, Voltage-Dependent, Open Channel *N*-Methyl-D-Aspartate Receptor Blocker

Chris G. Parsons and Kate Gilling

Summary

Electrophysiological techniques can be used to great effect to help determine the mechanism of action of a compound. However, many factors can compromise the resulting data and their analysis, such as the speed of solution exchange, expression of additional ion channel populations including other ligand-gated receptors and voltage-gated channels, compounds having multiple binding sites, and current desensitization and rundown. In this chapter, such problems and their solutions are discussed and illustrated using data from experiments involving the uncompetitive *N*-methyl-D-aspartate (NMDA) receptor antagonist memantine. Memantine differs from many other NMDA receptor channel blockers in that it is well tolerated and does not cause psychotomimetic effects at therapeutic doses. Various electrophysiological parameters of NMDA-induced current blockade by memantine have been proposed to be important in determining therapeutic tolerability, potency, onset and offset kinetics, and voltage dependency. These were all measured using whole cell patch-clamp techniques using hippocampal neurons. Full results are shown here for memantine, and these are summarized and compared with those from similar experiments with other NMDA channel blockers. The interpretation of these results is discussed, as are theories concerning the tolerability of NMDA channel blockers, with the aim of illustrating how electrophysiological data can be used to form and support a physiological hypothesis.

Key Words: NMDA; uncompetitive; concentration dependence; concentration clamp; voltage dependence; kinetics.

1. Introduction

Memantine is an uncompetitive *N*-methyl-D-aspartate (NMDA) receptor antagonist that is registered in Europe and the United States for the treatment of moderate to severe Alzheimer's disease (AD). It has clear symptomatic effects in both AD patients (1,2) and animal models of AD (3) and, on the basis of its mechanism of action, is also likely to show neuroprotective activity in AD (3,4). This compound blocks the channel in an use-dependent manner, meaning that it can only gain access to the channel in the presence of agonist, and remains trapped in the channel following removal of agonist (3,5,6). Both the clinical tolerability and the symptomatic effects of memantine have been attributed to its fast blocking kinetics and strong voltage dependency (3,5–7). These properties have been characterized by numerous groups using whole cell patch-clamp recordings from primary cultures of hippocampal and cortical neurons (6,8–15). However, there are several factors that must be taken into account when performing such experiments to ensure the quality of the recordings and their analysis.

- Fast blocking kinetics can only be measured accurately when fast concentration-clamp techniques are used to apply antagonists. This is particularly problematic with primary cultures of hippocampal/cortical neurons due to their large dendritic arborization, the inability to lift such cells from the bottom of the dish, and resulting problems of buffered diffusion. Fluid-in-fluid fast concentration-clamp systems with relatively large application diameters, for example, theta glass stepping motor systems, are preferred over systems such as U-type application tubes with which offset kinetics cannot be addressed because there is no real “wash off” of compounds with the latter technique.
- The native cells used probably have mixed receptor populations (for example, NR1a/2A and NR1a/2B), and differences in the potency of the antagonist at each of the receptor subtypes may exist. Uncompetitive antagonists such as memantine may also bind to multiple sites within the NMDA receptor channel (14,15). Both of these aspects can lead to double exponential blocking/unblocking kinetics that first become apparent when fast concentration-clamp techniques are used. When present, these double kinetics must be measured accurately and subsequently analyzed. In addition, the unblocking kinetics are voltage dependent, and this aspect cannot be addressed by using ramping protocols in voltage-dependency experiments (see below).
- Voltage-dependency experiments are often hampered by the presence of additional voltage-gated ion channels, and their contribution to the currents recorded must be minimized and/or accounted for in the analysis. One way around this problem is to use tetrodotoxin (TTX) to block voltage-activated sodium channels (VASCs) and replace K^+ with Cs^+ in the recording solutions to reduce the effects

Memantine as an Example

17

AQ2

01 of voltage-activated potassium channels (VAKCs). The contribution of voltage-
02 activated calcium channels on the currents measured can be reduced by lowering
03 Ca^{2+} in the extracellular solution (see **below**). The contribution of all voltage-
04 activated channels (VACs) can also be reduced by avoiding the use of relatively
05 fast ramping protocols and rather recording individual NMDA-induced currents
06 after holding at different holding potentials and allowing the VACs to desensitize/inactivate for several
07 **10s** of seconds following each incremental depolarizing step. For example, shifting the holding potential from -90 to $+70$ mV in steps of
08 10 mV, allowing at least 30 s at each new holding potential before applying agonist. Residual VAC currents can then be subtracted from the agonist-induced currents mediated through ligand-gated channels such as the NMDA receptor channel. However, such protocols are long and are associated with other potential problems (see **below**).

AQ3

AQ4

AQ5

13 • NMDA receptors show various forms of Ca^{2+} -dependent desensitization (with time constants of 500 ms to several seconds) (**16–18**), the presence of which can interfere with experiments assessing the blocking kinetics of open channel blockers such as memantine. This problem can be minimized by decreasing Ca^{2+} concentrations in the solutions used (see also **above**), but Ca^{2+} is an important cation for membrane stability. One way around this additional problem is to reduce Ca^{2+} concentrations in the presence of agonist (0.2 mM) but maintain normal Ca^{2+} concentrations (1.5 mM) between agonist applications to allow the cell membrane to “recover” between agonist applications.

AQ6

21 • Glycine is a co-agonist for NMDA receptors (at the glycine_B site) with an EC_{50} of around 1 μM , and its presence is a prerequisite for receptor channel activation by glutamate or NMDA (**19**). At non-saturating glycine concentrations, NMDA receptors show strong glycine-dependent desensitization, with quite fast kinetics ($\tau = 100\text{--}400$ ms), which can impede the analysis of antagonist blocking kinetics (**20**). Moreover, glycine concentrations in the solutions can be dynamically altered by the presence of microbial organisms in the perfusion setup as glycine is involved in metabolism. As such, the magnitude and rate of glycine-sensitive desensitization can change during long recordings, and it is essential to keep the whole perfusion system very clean. D-Serine is also a co-agonist for the glycine site (**21**), but it is not metabolized so easily and is the preferred co-agonist for such experiments, used at saturating concentrations. Clean perfusion systems are nonetheless very important for such experiments, for example, contamination with previously used “sticky” (most often lipophilic) compounds should be avoided.

34 • Aside from the various forms of receptor desensitization detailed **above**, NMDA receptors also show moderate rundown that should be minimized by the choice of appropriate intracellular (**ATP** regenerating) and extracellular (low Ca^{2+}) solutions. However, some form of run-down compensation is essential in the analysis to account for such dynamic changes, especially when assessing the potency of antagonists with several concentrations being tested sequentially over time.

AQ7,8

01 Most scientific papers on patch-clamp experiments tend to minimize the
02 description of the methods used, and minor details that could be very important
03 for the final outcome are often not apparent from such descriptions. The aim of
04 this chapter is to describe, in detail, the methods used to address such aspects
05 for memantine as an example of a fast, voltage-dependent, NMDA receptor
06 channel blocker.

07 **2. Materials**

08 **2.1. Cell Culture**

- 09 1. Mg²⁺-free Hanks' buffered salt solution (Gibco BRL, Germany) stored at 2–5°C
10 and warmed to approximately 35°C before use.
- 11 2. Solution of 0.05% DNase and 0.3% ovomucoid (Sigma Aldrich, Germany) in
12 phosphate-buffered saline (PBS, Gibco BRL) stored at –20°C and warmed to
13 approximately 35°C before use.
- 14 3. Solution of 0.66% Trypsin and 0.1% DNAase (Sigma Aldrich) in PBS stored
15 at –20°C and warmed to approximately 35°C before use.
- 16 4. Minimum essential medium (Gibco BRL) stored at 2–5°C and warmed to approx-
17 imately 35°C before use.
- 18 5. Poly-D-L-ornithine (500 µg/ml) dissolved in 0.5 M boric acid (both from Sigma
19 Aldrich), stored at –20°C, and warmed to approximately 35°C before use.
- 20 6. Laminin (Sigma Aldrich) dissolved in PBS to a concentration of 10 µg/ml, stored
21 at –20°C, and warmed to approximately 35°C before use.
- 22 7. NaHCO₃/HEPES-buffered minimum essential medium supplemented with 5% fetal
23 calf serum and 5% horse serum (all from Gibco BRL), stored at 2–5°C, and warmed
24 to approximately 35°C before use.
- 25 8. Cytosine-β-D-arabinofuranoside (Sigma Aldrich) stored at 2–5°C.
- 26 9. Plasticware including flasks, Petri dishes, and pipettes (Corning Incorporated,
27 Germany).

28 **2.2. Patch Clamp**

- 29 1. Borosilicate glass for recording pipettes with an outer diameter of 1.5 mm and an
30 inner diameter of 1.275 mm (Hilgenberg GmbH, Germany; cat. no. 1408411).
- 31 2. The P-97 horizontal pipette puller (Sutter Instruments, USA).
- 32 3. Square-walled application pipette glass with a wall-to-wall measurement of
33 700 µm (Warner Instruments LLC, USA; cat. no. P/N 3SG700-5).
- 34 4. The SF-77B Perfusion Fast-Step: a stepper motor-driven, double-barreled theta
35 glass application pipette delivery system (Warner Instruments LLC).
- 36 5. Silicon-glass tubing with an external diameter of 0.43 mm and an internal diameter
37 of 0.32 mm (S.G.E. GmbH, Germany).
- 38 6. Polyethylene tubing of the PE-10 size (Clay Adams, USA).
- 39 7. Low-volume manifolds (MM series six-port manifolds; Warner Instruments LLC).

- 01 8. Manifold valves (Lee Hydraulische Miniaturkomponenten GmbH, Germany; cat.
02 no. LFAA1201718H).
- 03 9. TIB 14S digital output trigger interface (HEKA, Germany).
- 04 10. EPC-9 or EPC-10 amplifier (HEKA).
- 05 11. Axiovert 35 inverted microscope (Carl Zeiss, Germany).
- 06 12. A valve driver, similar to those produced by Lee (Lee Hydraulische Miniaturkom-
07 ponenten GmbH; cat. no. IECX0501500A).
- 08 13. Software for data acquisition and analysis, such as TIDA 5.0 (HEKA), Excel 2000
09 (Microsoft, USA), and GraFit 5.0 (Erithacus Software Ltd., UK), and suitable
10 computer hardware.
- 11 14. Intracellular solution used for recording NMDA receptor-mediated currents from
12 hippocampal neurons, consisting of 120 mM CsCl, 10 mM EGTA, 1 mM MgCl₂,
13 0.2 mM CaCl₂, 10 mM glucose, 20 mM tetraethyl ammonium chloride, 2 mM
14 ATP, and 0.2 mM cAMP. All these components were purchased from Sigma
15 Aldrich and stored according to manufacturer's instructions. AQ9
- 16 15. Extracellular bath solution used for recording NMDA receptor-mediated currents
17 from hippocampal neurons, consisting of 140 mM NaCl, 3 mM CsCl, 10 mM
18 glucose, 10 mM HEPES, 0.2 mM CaCl₂, and 4.5 mM sucrose, and supplemented
19 with 0.35 μM TTX. All these components were purchased from Sigma Aldrich
20 and stored according to manufacturer's instructions.
- 21 16. NMDA (Sigma Aldrich) stored as a 100 mM stock solution in distilled water
22 at -20 °C. The stock solution of the co-agonist D-serine (Sigma Aldrich) prepared
23 and stored under the same conditions but at a concentration of 10 mM.
- 24 17. The NMDA receptor antagonists memantine, neramexane (Merz Pharmaceuticals
25 GmbH, Germany), ketamine, PCP, dextromethorphan, and dextrorphan (Sigma
26 Aldrich) all stored in distilled water at 2-5 °C as stock solutions of 10 mM. AQ10

27 3. Methods

28 3.1. Cell Culture

29 Hippocampal tissue was obtained from rat embryos (E20-E21) and was then
30 transferred to Ca²⁺- and Mg²⁺-free Hanks' buffered salt solution on ice. Cells AQ11
31 were mechanically dissociated in 0.05% DNAase/0.3% ovomucoid solution
32 following an 8-min pre-incubation with 0.66% Trypsin/0.1% DNAase solution.
33 The dissociated cells were then centrifuged at 18 g for 10 min, re-suspended in
34 minimum essential medium, and plated at a density of 150,000 cells/cm² onto
35 poly-D-L-ornithine/laminin-precoated plastic Petri dishes. These dishes were
36 precoated by treating dishes overnight at 37 °C with poly-D-L-ornithine, washing
37 twice with PBS, and then incubating with laminin solution overnight at 37 °C.
38 Excess solution was aspirated and dishes washed with PBS followed by the cell
39 medium before cell plating. The cells were nourished with NaHCO₃/HEPES-
buffered minimum essential medium supplemented with 5% fetal calf serum AQ12

01 and 5% horse serum and incubated at 37°C with 5% CO₂ at 95% humidity.
02 The medium was exchanged completely following the inhibition of further glial
03 mitosis with cytosine-β-D-arabino-furanoside after about 5 days in vitro (DIV).
04 Patch-clamp recordings were made after 12–15 DIV.

05 **3.2. Patch Clamp**

06 *3.2.1. Recording*

08 Voltage-clamp recordings were made in the whole cell configuration of
09 the patch-clamp technique at a holding potential of –70 mV, unless otherwise
10 stated. All recordings were made at room temperature (20–23°C) (Note: The
11 kinetics of drug/receptor interactions are highly dependent on temperature.)
12 Pyramidal cells were visualized using an inverted microscope under phase
13 contrast and selected for patching based upon their position and morphology.
14 The cells were opened by suction after the formation of a giga seal between
15 the pipette and cell membrane and were allowed to stabilize for 1–2 min before
16 recordings were made. Patch-clamp pipettes were pulled from borosilicate
17 glass using a horizontal puller and, when filled with intracellular solution, had
18 resistances of 1–3 MΩ. Currents were recorded using an EPC-9/10 amplifier,
19 and TIDA 5.0. software was used for the collection and storage of data. For
20 full details of the functions, measurements, and compensations performed by
21 the EPC-9/10 amplifier and related software *see refs. 22,23*. Briefly, offset
22 compensation was performed for each open pipette in order to ensure that the
23 command potential is equal to the membrane potential. The liquid junction
24 potential was measured for each set of solutions using an agar bridge in place of
25 the usual silver chloride pellet as the ground electrode. Liquid junction potential
26 was measured by filling one perfusion chamber with intracellular solution as the
27 reference and the other chamber with extracellular solution. For the solutions
28 used for recording from the hippocampal neurons, the liquid junction potential
29 was measured to be 3.4 mV.

30 Series resistance was measured (mean value of 4.22 ± 0.14 MΩ) and accord-
31 ingly compensated for in conjunction with capacitance. Fast capacitive currents
32 were corrected for by the EPC-9/10 upon formation of the giga seal, and whole
33 cell capacitance correction was performed after the cell was opened. These
34 procedures were performed semi-automatically using the amplifier and TIDA
35 5.0 software.

36 The current signal was filtered by the EPC-9/10 amplifier using the three-
37 pole prefilter with Bessel 10 kHz bandwidth and the four-pole filter set to
38 2.9 kHz with Bessel characteristic. Current measurements were acquired at a
39 rate of 10 kHz to avoid potential problems of aliasing.

01 3.2.2. Perfusion System

02 Test substances were applied by switching channels of a modified stepper
03 motor-driven, double-barreled theta glass application pipette. The openings of
04 the square-walled application pipette glass were reduced to 200–250 μM by
05 pulling these glass capillaries, by hand, over a Bunsen burner and then cleanly
06 separating “two” new perfusion pipettes by cutting them with a diamond cutter.
07 Furthermore, the internal dead volume of such application pipettes was reduced
08 to a minimum by the following procedure. Silicon-glass tubing was inserted as
09 far as possible toward the tips of the theta glass application “pipettes” (around
10 2–3 mm from the tip). The non-tip, open ends of the silicon-glass tubing was
11 blocked with acrylic glue, and the pipettes were then reverse filled with molten
12 wax almost to the open tips of the silicon-glass tubing. After this procedure,
13 wax was cleaned from the outside of the perfusion pipettes, and the glued ends
14 of the silicon-glass tubing were cut free and attached through conventional
15 polyethylene tubing to the low volume six-port manifolds. These manifolds
16 were then connected to an automatic perfusion array gated through manifold
17 valves to gravity-fed syringes containing the solutions of interest. Perfusion
18 was controlled using the TIB 14S digital output trigger interface in conjunction
19 with the EPC-9/10 and the TIDA data acquisition system. Valves were driven
20 by a custom-made valve driver to provide the necessary power (490 mW per
21 valve) and spiked voltage jumps. Twenty volts for 10 ms then held at 10 V.

AQ13

22 Optimal positioning of the pipette was practiced using solutions of different
23 osmolarity to visualize the interface between solutions under phase-contrast
24 microscopy. The best angle was found to be 45°, and care was taken to keep
25 the lower edge of the application pipette tip parallel to, and as close as possible
26 to, the bottom of the dish without scratching the plastic during the stepping
27 motor movement. The lower edge of the application pipette was positioned with
28 the start channel centered some 150–250 μM from the neuron of interest. The
29 solution exchange time of this perfusion system as measured using small, lifted
30 cells was approximately 20 ms. Complete exchange of the perfused solutions
31 to be applied through the application pipette was of the order of 1–2 s. The
32 level of bath solution was kept constant using a vacuum-driven glass suction
33 pipette. This is important to avoid changes in recording pipette capacitive
34 characteristics.

36 3.2.3. Solutions

38 The composition of the intracellular solution used when recording NMDA
39 receptor mediated from hippocampal neurons is given in **Subheading 2.2.14.**

AQ14

AQ15

01 The absence of intracellular K^+ and the presence of intracellular TEA should
02 block VAKCs. ATP and cAMP were included to decrease rundown although
03 more elaborate ATP regenerating systems can be used for more problematic
04 receptors such as neuronal nicotinic receptors (24). The corresponding extra-
05 cellular bath solution composition is given in **Subheading 2.2.15**. TTX was
06 included at $0.35 \mu M$ in order to block VASCs, and D-serine was present at
07 $10 \mu M$ in all extracellular solutions—this concentration being sufficient to
08 saturate the glycine_B site, which should remain stable during the course of the
09 experiments.

10 3.2.4. Cumulative Protocols

11
12 Cumulative protocols can be used for faster determination of concentration
13 dependency of blockade and were shown to produce very similar IC_{50} deter-
14 minations as kinetic protocols (see **Table 1**). In these protocols, five to six
15 sequentially increasing concentrations (in a log 3 progression, for example, 0.3,
16 1, 3, 10, and $30 \mu M$) of memantine or other standard uncompetitive NMDA
17 receptor antagonists are applied in a cumulative regime, each for 10–30 s, in the
18 continuous presence of NMDA ($200 \mu M$) for 100–200 s, and recovery is only
19 recorded after the last and highest concentration. With such protocols, cells do
20 not have to remain stable for such long recording durations. However, they give
21 little useful information on the kinetics of block, and desensitization/rundown
22 is more of a problem.

23 3.2.5. Kinetic Experiments

24
25 Kinetic experiments were performed by applying various single concentra-
26 tions of memantine or standard uncompetitive NMDA receptor antagonists for
27 10–30 s in the continuous presence of NMDA ($200 \mu M$) for 30–120 s. When
28 using this protocol, currents are allowed to recover after each application of
29 antagonist, and onset and offset kinetics can be measured.

30 3.2.6. Voltage Dependency

31
32 Fractional block of currents by memantine ($10 \mu M$) at various holding poten-
33 tials was used to determine the voltage dependency of this effect. The holding
34 potential was changed every 120 s from -80 to $+60$ mV in 10 mV incre-
35 ments, and NMDA ($200 \mu M$) was applied for 41 s at each holding potential.
36 Memantine ($10 \mu M$) was applied for 11 s during each NMDA application
37 period. During the recovery period, 15 s following the removal of memantine,
38 neurons were clamped to $+70$ mV for 5 s in the continuing presence of NMDA
39 to facilitate complete recovery from antagonism. Similar experiments were

AQ16

01
02
03
04
05
06
07
08
09
10
11
12
13
14
15
16
17
18
19
20
21
22
23
24
25
26
27
28
29
30
31
32
33
34
35
36
37
38
39

Table 1
Summary of the Results From Experiments Measuring the Antagonistic Properties of Various Known N-Methyl-D-Aspartate (NMDA) Receptor Antagonists Against NMDA-Induced Currents Recorded From *Xenopus* Oocytes and Cultured Hippocampal Neurons

Substance	Cumulative IC_{50} (μ M)	Cumulative Hill	Kinetic IC_{50} (μ M)	Kinetic Hill	K_{on} (10^4 M/s)	K_{off} (per second)	K_d (μ M)	IC_{50} (0 mV) (μ M)	δ	β
Memantine	1.87 \pm 0.17	0.80 \pm 0.04	1.27 \pm 0.08	0.93 \pm 0.06	5.94 \pm 0.35	0.125 \pm 0.019	2.100 \pm 0.450	17.35 \pm 1.78	0.83 \pm 0.04	0.08 \pm 0.02
Neramexane	1.21 \pm 0.04	0.88 \pm 0.02	0.85 \pm 0.05	0.81 \pm 0.03	9.30 \pm 0.90	0.120 \pm 0.008	1.330 \pm 0.200	16.99 \pm 2.09	0.96 \pm 0.04	0.10 \pm 0.03
Ketamine	1.47 \pm 0.22	0.82 \pm 0.08	0.98 \pm 0.09	1.01 \pm 0.08	3.95 \pm 0.50	0.070 \pm 0.005	1.670 \pm 0.320	13.16 \pm 0.90	0.85 \pm 0.05	0.08 \pm 0.02
PCP	0.13 \pm 0.01	0.78 \pm 0.08	0.11 \pm 0.03	0.70 \pm 0.05	7.00 \pm 0.19	0.010 \pm 0.003	0.143 \pm 0.004	1.26 \pm 0.11	0.65 \pm 0.04	0.10 \pm 0.17
Dextromethorphan	1.95 \pm 0.17	1.37 \pm 0.15	2.11 \pm 0.17	1.16 \pm 0.10	1.74 \pm 0.16	0.127 \pm 0.027	7.470 \pm 1.820	15.34 \pm 1.51	0.84 \pm 0.05	0.14 \pm 0.02
Dextrorphan	0.34 \pm 0.05	1.02 \pm 0.10	0.36 \pm 0.08	1.00 \pm 0.17	19.90 \pm 0.78	0.063 \pm 0.004	0.317 \pm 0.023	3.39 \pm 0.70	0.61 \pm 0.06	-0.01 \pm 0.14
Mg ²⁺	NC	NC	37.62 \pm 1.41	0.82 \pm 0.02	11.28 \pm 0.75	21.61 \pm 0.60	191.6 \pm 13.8	5521 \pm 261	0.95 \pm 0.02	-0.32 \pm 0.01

NC, not calculated.

Only compounds produced by Merz Pharmaceuticals GmbH were tested using *Xenopus* oocytes. The hippocampal IC_{50} and Hill coefficient values and onset and offset kinetics are calculated from recordings in which the NMDA currents were allowed to recover between the application of various concentrations on antagonist. All data are shown in the form of value \pm SE.

01 performed with PCP, dextrorphan, and (+)MK-801 except that the appli-
02 cation and recovery times had to be increased for these very slow channel
03 blockers.

04 In order to subtract any residual VAC currents, mirror voltage-clamp (P5)
05 protocols with smaller (20%) voltage steps in the opposite direction were
06 run between agonist and antagonist applications at each holding potential,
07 for example, the equivalent for a step from -90 to $+70$ mV (difference
08 of -160 mV) was -90 to -122 mV (difference of -32 mV).
09

10 3.2.7. Analysis of Data

11 TIDA 5.0 software was used for the quantification of individual current
12 amplitudes and kinetics. Excel 2000 was used to pool these data and GraFit 5.0
13 software used to fit pharmacological equations and pooled kinetic K_{on} and K_{off}
14 values. For all data points, the value given is the mean of results from four to
15 eight cells per concentration.
16

17 Rundown was usually not extreme for these NMDA receptor currents
18 recorded from cultured hippocampal neurons (normally less than 10% over
19 a 1-min period in the continuous presence of agonist). However, in order
20 to produce the most accurate assessment of potency, the analysis never-
21 theless corrected for extrapolated linear current rundown—this was increas-
22 ingly important for high-affinity compounds where the duration of the agonist
23 exposure was prolonged to assure that low concentrations of antagonist reached
24 steady-state blockade. Antagonism of NMDA receptor-mediated currents was
25 measured as the magnitude of the steady-state blocked current as a percentage
26 of the control current. For non-kinetic antagonistic protocols with five cumula-
27 tively increasing concentrations of antagonist, the control current for each
28 antagonist concentration was calculated by a linear projection from the
29 steady-state current before and after antagonist application, that is, for the
30 first antagonist concentration, control current = $0.85 \times$ current before antag-
31 onist + $0.15 \times$ recovery current. For the second antagonist concentration, these
32 same currents were multiplied by 0.7 and 0.3, respectively, and so on for
33 all concentrations. For kinetic protocols, single concentrations of antagonist
34 were applied in the continuing presence of agonist, and the control current
35 was taken as the mean of the steady-state current before and after antagonist
36 application.

37 Potency of compounds was assessed by plotting the mean percentage current
38 magnitude, calculated with standard error against antagonist concentration, and
39 a curve was fit using the logistic equation for which the variable parameters

01 IC_{50} and Hill coefficient (n) were free and the range and background values
 02 were normally set to 100 and 0, respectively;

$$03 \quad \% \text{ current} = \frac{\text{range}}{1 + (\text{antagonist}/IC_{50})^n} + \text{background.} \quad (1)$$

06 For kinetic protocols, exponential fits to both onset and offset kinetics were
 07 made using TIDA 5.0 software, and most onset and offset responses were often
 08 well fit by a single exponential function, where a and b are current amplitudes
 09 and c represents the time constant, τ :

$$11 \quad \text{amplitude} = a + b \cdot e^{\text{time}/c}. \quad (2)$$

13 When double exponential fits described the data better, these were fit with
 14 the following equation:

$$16 \quad \text{amplitude} = a + b \cdot e^{\text{time}/c} + d \cdot e^{\text{time}/f}, \quad (3)$$

18 where a , b , and d are current amplitudes and c and f are time constants
 19 (c represents τ_{fast} and f is τ_{slow}). These were then integrated to produce a single
 20 time constant (t_{combined}) according to **Eq. 4**.

$$22 \quad t_{\text{combined}} = \frac{[c \cdot b / (b + d)] + [f \cdot d / (b + d)]}{[b / (b + d)] + [d / (b + d)]}. \quad (4)$$

24 The rationale for this weighting procedure was to allow simple comparison
 25 between the rate kinetics produced by this investigation and also with previous
 26 data for memantine and other channel blockers for which similar techniques
 27 or simple single exponentials were used to fit the data. Another reason for this
 28 weighting was to allow a simple calculation of calculated K_d (see **Eq. 6**).

29 Mean values of the time constant (τ) were calculated for each concentration
 30 of antagonist, and $1/\tau$ was plotted against concentration. These data were fit using
 31 linear equations, where m is the gradient of the line, which corresponds to K_{on}
 32 for the onset rate fit, and g is the intercept at the y axis, which corresponds to
 33 K_{off} for the offset rate fit:

$$35 \quad y = m \cdot x + g. \quad (5)$$

37 All compounds tested showed concentration-dependent open channel
 38 blocking kinetics, whereas the offset rate was essentially concentration
 39 independent. As expected, the fit of τ_{on} against concentration intercepted the y

01 axis at similar values to the fit of τ_{off} against concentration. Calculation of the
 02 ratio $K_{\text{off}}/K_{\text{on}}$ was used to reveal an apparent K_d that was then compared with
 03 the IC_{50} calculated at equilibrium:

$$04 \quad K_d = \frac{K_{\text{off}}}{K_{\text{on}}}. \quad (6)$$

07 To assess voltage dependency, single concentrations of antagonist were
 08 applied to currents in the plateau phase and then the cell was allowed to recover
 09 before stimulation was repeated at a more positive holding potential (holding
 10 potential was increased by increments of +10 mV each time). Blockade was
 11 expressed as a percentage of the mean control current recorded before and after
 12 the application of antagonist, as in the kinetic experiments **described above**.
 13 The pooled data were then fit by the following equation, where $IC_{50}(0)$ is the
 14 IC_{50} at 0 mV, β is the fraction of voltage-independent sites, δ is the fraction of
 15 the electric field sensed by the voltage-dependent site, and all other parameters
 16 have their normal meaning (z , valency; F , Faraday's constant; R , universal gas
 17 constant; and T , absolute temperature):

$$18 \quad \text{fractional current} = \frac{1 - \beta}{19 \quad [1 + \text{antagonist}] / [IC_{50}(0) \cdot e^{-z\delta FV/RT}]} \quad (7)$$

20 21 22 4. Results

23 The application of NMDA (200 μM) in the continuous presence of D-serine
 24 (10 μM) to hippocampal neurons evoked currents that were attenuated by all
 25 the uncompetitive NMDA receptor antagonists used in this study. The data are
 26 summarized in **Table 1**.

27 28 4.1. Potency

29 Initial experiments involved the application of five sequentially increasing
 30 concentrations of antagonist. However, kinetic measures of both onset and
 31 offset rates for each concentration of antagonist cannot be determined using
 32 this application protocol, so the kinetic protocol was employed that involved
 33 the application of antagonist in the continuous presence of NMDA and D-serine
 34 with a period of current recovery between each antagonist concentration. This
 35 protocol could also be considered to give more accurate measure of potency,
 36 as the magnitude of blockade by each concentration is assessed compared with
 37 the current before and after each application of antagonist, but the difference
 38 between values determined from each set of results is clearly only slight
 39 (*see Table 1*).

AQ17

01 Memantine antagonized NMDA currents concentration-dependently with an
02 IC_{50} value of $1.87 \pm 0.17 \mu M$ and a Hill coefficient of 0.80 ± 0.04 when the
03 cumulative protocol was used (see Fig. 1). From the data produced using the
04 kinetic protocol, as shown in Fig. 1B, a new concentration-response curve was
05 produced, and the IC_{50} value calculated from this curve was only marginally
06 lower ($1.27 \pm 0.08 \mu M$) although the difference does reach a level of signifi-
07 cance ($p = 0.019$, $t = 3.19$; Student's t -test using raw data). The Hill coefficient
08 is slightly higher (0.93 ± 0.06) than that derived from the earlier data, but values
09 derived using these two protocols are not significantly different ($p > 0.05$;
10 Student's t -test using raw data).

11 4.2. Kinetics

12
13 Simple analysis of the kinetic data shows memantine to have concentration-
14 dependent blocking and concentration-independent unblocking kinetics ($K_{on} =$
15 $5.94 \pm 0.35 \times 10^4 M/s$ and $K_{off} = 0.125 \pm 0.019$ per second). From these values,
16 K_d can be calculated as $2.10 \pm 0.45 \mu M$ according to the equation $K_d =$
17 K_{off}/K_{on} , which correlates well with the IC_{50} values calculated by both of the
18 concentration-response curves.

19 However, memantine did indeed sometimes show double exponential
20 kinetics (see Fig. 2). The onset and offset kinetics of blockade following
21 concentration jumps with memantine ($10 \mu M$ at $-70 mV$) showed double
22 exponential kinetics: τ_{on} fast $86.9 \pm 6.3 ms$ (64.7%); τ_{on} slow $1383 \pm 122 ms$;
23 τ_{off} fast $834 \pm 321 ms$ (22.9%); and τ_{off} slow $4795 \pm 921 ms$. It should be noted
24 that the kinetics of blockade by memantine in these experiments with D-
25 serine ($10 \mu M$ at $-70 mV$) were somewhat faster than those using glycine at a
26 subsaturating concentration ($1 \mu M$ at $-70 mV$) (12). This is not surprising as
27 channel gating kinetics also influence the kinetics of open channel blockade.
28 The relief of blockade following voltage jumps to $+70 mV$ in the continuous
29 presence of memantine ($10 \mu M$) also showed rapid, double exponential kinetics:
30 τ_{off} fast $98.7 \pm 38.1 ms$ (43.9%) and τ_{off} slow $725 \pm 122 ms$. Reblock by
31 memantine following jumps back to $-70 mV$ was extremely fast: τ_{on} fast
32 $7.7 \pm 2.2 ms$ (41.6%) and τ_{on} slow $285 \pm 41 ms$. The extremely rapid reblock by
33 memantine and additional minor effects of such voltage steps on the kinetics
34 of NMDA currents in the absence of antagonist necessitated fitting responses
35 with memantine as the ratio between responses in the presence/absence of
36 memantine. The difference in onset kinetics between the concentration-clamp
37 and voltage-step protocols may be explained by a second, extracellular holding
38 site for memantine on the NMDA receptor (3). Alternatively, it may just indicate
39 that the concentration clamp was not fast enough.

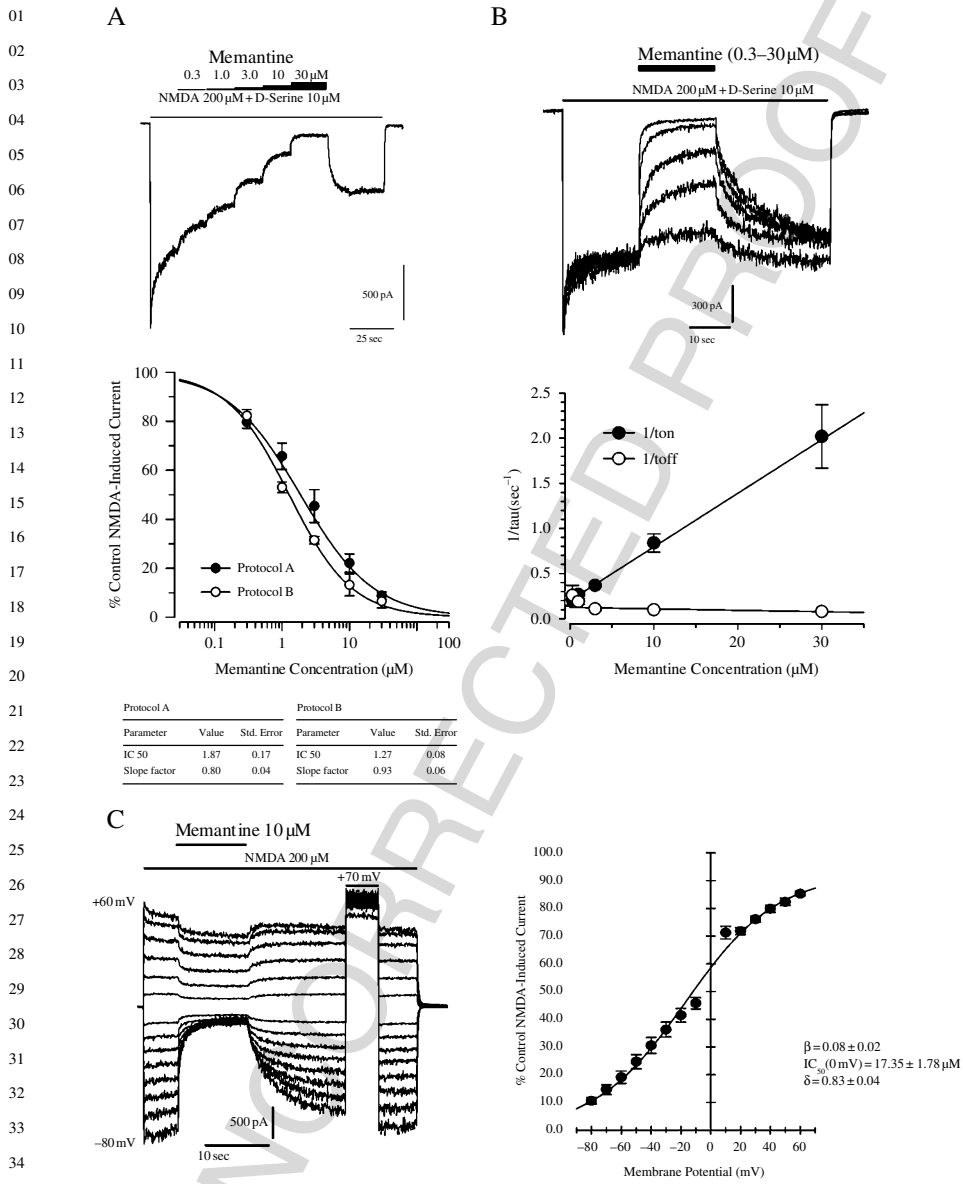


Fig. 1. Antagonism of *N*-methyl-D-aspartate (NMDA) currents recorded from cultured hippocampal neurons by memantine. (A) Stepwise application of increasing concentrations of antagonist during constant application of agonists. Mean rundown-corrected percentage blockade (\pm SE) was plotted against antagonist concentration

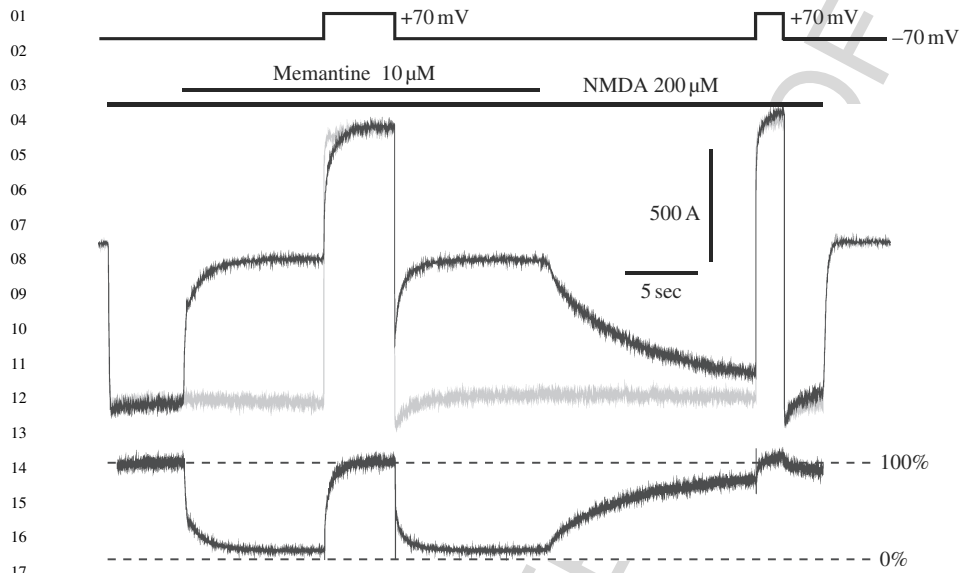


Fig. 2. Double exponential kinetics of blockade by memantine in cultured hippocampal neurons. Traces are averages of 10 recordings, and residual capacitive artifacts were subtracted. The bottom trace was constructed by basing recordings in the presence of memantine (black) as a percentage of those in the absence of memantine (gray). This was then used to fit the kinetics of the data. NB: Neurons were shortly clamped to +70 mV during the memantine washout phase to facilitate recovery.

Fig. 1. on a logarithmic scale and the curve fit using Eq. 1 (filled circles). (B) Attenuation of currents by memantine (0.3–30 μM) with current recovery between antagonist applications. Mean control-corrected percentage blockade ($\pm\text{SE}$) was plotted against antagonist concentration on a logarithmic scale and the curve fit using Eq. 1 (open circles). The onset and offset kinetics followed a single or double exponential time course. Mean $1/t$ values ($\pm\text{SE}$) were plotted against antagonist concentration and fit according to Eq. 5 from which K_{on} and K_{off} were read. These two values were then used to calculate K_{d} . (C) Voltage dependence of antagonism of the NMDA currents by a single concentration of memantine (10 μM). The initial holding potential of -80 mV was increased for each stimulation in increments of 10 mV until it reached $+60$ mV. In the example recording shown, it can be seen that a voltage step to $+70$ mV was added during current recovery, but this was not deemed necessary for further experiments. The mean percentage blockade of control currents ($\pm\text{SE}$) was plotted against holding potential and fit using Eq. 7.

4.3. Voltage Dependency

Blockade of NMDA receptor-mediated currents by memantine was voltage dependent, as illustrated by the δ value of 0.83 ± 0.04 , and an approximately 10-fold higher IC_{50} value at 0 mV compared with -70 mV [$IC_{50}(0\text{mV}) = 17.35 \pm 1.78 \mu\text{M}$] (see Fig. 1C). The proportion of the voltage-independent sites, β , was very small (0.08 ± 0.02). To ensure that memantine had completely left the channel and the current was fully recovered, a 5-s voltage step to $+70$ mV was added during the current recovery, as can be seen in the trace shown, but this was not considered necessary for subsequent experiments with moderate affinity blockers that show similar fast kinetics. However, such procedures can be very useful when determining the voltage dependency of more potent, slower blockers such as (+)MK-801 (3).

5. Notes: The Interpretation and Application of Electrophysiological Data

The reason for the better therapeutic safety of memantine compared with other channel blockers such as (+)MK-801 and phencyclidine is still a matter of debate, and data such as those presented in this chapter (summarized in Table 1) have been utilized to support several theories. The interpretation of these electrophysiological data and how they have been used to form hypotheses concerning actions of compounds in vivo are described in the following notes.

1. Memantine and other well-tolerated open channel blockers such as amantadine, dextromethorphan, ARL 15896AR, and ADCI show much faster open channel blocking/unblocking kinetics than compounds burdened with negative psychotropic effects such as (+)MK-801 or phencyclidine (3,6,7,10,25,26). The kinetics of (+)MK-801 and phencyclidine are too slow to allow them to leave the channel upon depolarization, which is reflected in apparently weaker voltage dependency. These two parameters are directly related to affinity, with lower affinity compounds such as memantine showing faster kinetics and apparently stronger voltage dependency, as reflected in estimated δ value (13). The δ value describes the percentage of the transmembrane field the drug experiences when blocking the NMDA receptor channel (3). The unblocking rate of memantine in the continuous presence of this antagonist following depolarizing voltage steps is very rapid and well within the time course of an NMDA receptor-mediated EPSP.
2. Memantine blocks and unblocks open NMDA receptor channels with double exponential kinetics. The amplitude and speed of the fast component of block increases with memantine concentration. In contrast, the speed of fast unblock remains constant, but the amplitude decreases with memantine concentration (8,9,14,15,27). Moreover, the predominant effect of depolarization is to increase

AQ18

AQ19,20

AQ21

- 01 dramatically the weight of the faster recovery time constant (9,11,27). These data
02 indicate that memantine binds to at least two sites within the channel (14,15).
- 03 3. Both Lipton's and Rogawski's groups have proposed that the ability of low-affinity
04 open channel blockers to gain rapid access to the NMDA receptor channel is
05 important in determining their therapeutic safety in ischemia and epilepsy (7,26,28).
06 However, this hypothesis alone cannot explain the better therapeutic profile of
07 memantine as, even if receptors are only blocked following pathological activation,
08 they would then remain blocked in the continuous presence of memantine, and
09 therefore be unavailable for subsequent physiological activation. Physiologically,
10 NMDA receptors are transiently activated by millimolar concentrations of glutamate
11 (29) following strong depolarization of the postsynaptic membrane that rapidly
12 relieves their voltage-dependent blockade by Mg^{2+} (30), whereas during patho-
13 logical activation, NMDA receptors are activated by lower concentrations of
14 glutamate but for much longer periods of time (31–36). Unfortunately, the voltage
15 dependency of the divalent cation Mg^{2+} is so pronounced that it also leaves
16 the NMDA channel upon moderate depolarization under pathological conditions.
17 Although uncompetitive antagonists also block the NMDA receptor channel, high-
18 affinity compounds such as (+)MK-801 have much slower unblocking kinetics
19 than Mg^{2+} and less pronounced functional voltage dependency and are therefore
20 unable to leave the channel within the time course of a normal NMDA receptor-
21 mediated excitatory postsynaptic potential. As a result, (+)MK-801 blocks both the
22 pathological and the physiological activation of NMDA receptors (3).
- 23 4. We were the first to suggest that the combination of fast offset kinetics and strong
24 voltage dependency allows memantine to rapidly leave the NMDA channel upon
25 transient physiological activation by millimolar concentrations of synaptic glutamate
26 but blocks the sustained activation by micromolar concentrations of glutamate under
27 moderate pathological conditions (6,12,13). This hypothesis is further supported
28 by the fact that although the predominant component of offset kinetics at near
29 resting membrane potentials is still too slow to allow synaptic activation—that is,
30 around 5 s—the relief of blockade in the continuous presence of memantine upon
31 depolarization is much faster due to an increase in the weight of the faster recovery
32 time constant (9,27,37,38). These kinetics are likely to be even faster in vivo owing
33 to higher temperatures (39). Furthermore, the rate of recovery from memantine
34 blockade is dependent on the open probability of NMDA channels (10) and therefore
35 would be faster in the presence of higher, synaptic concentrations of glutamate
36 (29). Given the crucial role of NMDA receptors in neuronal plasticity, the fact that
37 memantine improves cognition and neuronal plasticity seems paradoxical at the first
38 glance. It should be realized, however, that Mg^{2+} is an endogenous NMDA channel
39 blocker, and its removal from the channel leads both to an impairment in neuronal
plasticity (40,41) and a neuronal death (42). Any dysfunction of postsynaptic
neurons leading to weakened blockade by Mg^{2+} , for example, because of partial
depolarization as a consequence of an energy deficit, may trigger such functional

- (plasticity) and structural (neuronal loss) deficits (**4,43**). Because memantine is more potent and slightly less voltage-dependent than Mg^{2+} , it may thus serve as a more effective surrogate for Mg^{2+} (**6**). As a result of its somewhat less pronounced voltage dependency, memantine is more effective than Mg^{2+} in blocking tonic pathological activation of NMDA receptors at moderately depolarized membrane potentials. However, following strong synaptic activation, memantine like Mg^{2+} can leave the NMDA receptor channel with voltage-dependent, fast unblocking kinetics. In turn, memantine suppresses synaptic noise but allows the relevant physiological synaptic signal to be detected. This provides both neuroprotection and symptomatic restoration of synaptic plasticity by one and the same mechanism (**3,4**). Antagonists that have “too high” affinity for the channel or “too little” voltage dependence, such as dizocilpine [(+)-MK-801], thus produce numerous side effects as they essentially act as an irreversible plug of the NMDA receptor channel and block both pathological and physiological function.
5. A moderate potentiation of NMDA-induced outward currents by memantine at positive potentials in hippocampal neurons has also been reported (**11**) (data not shown here). This could be related to the finding that Mg^{2+} and ketamine increased NMDA receptor-mediated currents in cultured mouse hippocampal neurons and HEK-293 cells expressing NMDA $\xi 1/\epsilon 2$ receptors by increasing the affinity of the glycine_B site for the co-agonist (**44**). Such a facilitation would be predicted to be more pronounced with lower concentrations of glycine. This could have important functional implications as the differentiation between the block of NMDA receptors at near resting membrane potentials and the lesser block following strong synaptic depolarization to around -20 mV would be enhanced by such a mechanism and would facilitate the ability of memantine to differentiate between pathological and physiological activation of NMDA receptors. Such a potentiation was not seen in this study, most likely because of the use of saturating concentrations of D-serine.
 6. It should also be noted that a third theory was recently proposed in an excellent paper by Blanpied et al. (**8**) (*see* **ref. 5** for review) and supported by data from Sobolevsky et al. (**14**) (not shown here). The data indicate that memantine and amantadine appear to have a lesser tendency to be trapped in NMDA receptor channels than do phencyclidine or (+)-MK-801. This difference was attributed to the ability of channel blockers to increase the affinity of NMDA receptors for agonist and the faster kinetics of the amino adamantanes. Receptors blocked by memantine retain agonist and thereby open and release memantine following removal of both agonist and memantine from the extracellular solution (**10**). This partial trapping is less pronounced for higher affinity compounds as their slower unblocking kinetics do not allow them to leave the channel quickly enough following agonist removal. The relief of block in the absence of agonist was greater in the experiments of Sobolevsky et al. (**14**). This, however, may have been due to the use of higher concentrations of aspartate that would have increased the proportion of liganded receptors at the time of agonist/antagonist removal. Blanpied et al. (**8**) proposed

01 that partial trapping may underlie the better therapeutic profile of memantine as
02 a proportion of channels—around 15–20%—would always unblock in the absence of
03 agonist and thereby be available for subsequent physiological activation. In other
04 words, the antagonism by memantine is like that of a low intrinsic activity partial
05 agonist in that it does not cause 100% blockade of NMDA receptors. Although this
06 theory is attractive, it is only relevant for the therapeutic situation if partial trapping
07 also occurs in the continuous presence of memantine. This point had not been
08 addressed previously. This prompted us to perform experiments on partial trapping
09 in the continuing presence of memantine, and the results of these studies were very
10 similar to those reported by Blanpied et al. (8), that is, around 15% of channels
11 released memantine following agonist removal (3). However, although this theory
12 can be used to explain the therapeutic tolerability of memantine, it provides no
13 mechanism of action for the symptomatic effects observed in AD patients.

14 References

- 15 1. Reisberg, B., R. Doody, and H.J. Mobius (2003) Memantine in moderate-to-severe
16 Alzheimer's disease – reply. *The New England Journal of Medicine* **349**, 610–612.
- 17 2. Tariot, P.N., M.R. Farlow, G.T. Grossberg, S.M. Graham, S. McDonald, and
18 I. Gergel (2004) Memantine treatment in patients with moderate to severe
19 Alzheimer disease already receiving donepezil – a randomized controlled trial.
20 *Jama: The Journal of the American Medical Association* **291**, 317–324.
- 21 3. Parsons, C.G., W. Danysz, and G. Quack (1999) Memantine is a clinically
22 well tolerated N-methyl-D-aspartate (NMDA) receptor antagonist – a review of
23 preclinical data. *Neuropharmacology* **38**, 735–767.
- 24 4. Danysz, W. and C.G. Parsons (2003) The NMDA receptor antagonist memantine
25 as a symptomatological and neuroprotective treatment for Alzheimer's disease:
26 preclinical evidence. *International Journal of Geriatric Psychiatry* **18**, S23–S32.
- 27 5. Johnson, J.W. and S.E. Kotermanski (2006) Mechanism of action of memantine.
28 *Current Opinion in Pharmacology* **6**, 61–67.
- 29 6. Parsons, C.G., R. Gruner, J. Rozental, J. Millar, and D. Lodge (1993) Patch-clamp
30 studies on the kinetics and selectivity of N-methyl-D-aspartate receptor antag-
31 onism by memantine (1-amino-3,5-dimethyladamantan). *Neuropharmacology* **32**,
32 1337–1350.
- 33 7. Rogawski, M.A. (1993) Therapeutic potential of excitatory amino-acid antago-
34 nists – channel blockers and 2,3-benzodiazepines. *Trends in Pharmacological*
35 *Sciences* **14**, 325–331.
- 36 8. Blanpied, T.A., F.A. Boeckman, E. Aizenman, and J.W. Johnson (1997) Trapping
37 channel block of NMDA-activated responses by amantadine and memantine.
38 *Journal of Neurophysiology* **77**, 309–323.
- 39 9. Bresink, I., T.A. Benke, V.J. Collett, A.J. Seal, C.G. Parsons, J.M. Henley, and
G.L. Collingridge (1996) Effects of memantine on recombinant rat NMDA receptors
expressed in HEK 293 cells. *British Journal of Pharmacology* **119**, 195–204.

AQ22

- 01 10. Chen, H.S.V. and S.A. Lipton (1997) Mechanism of memantine block of NMDA-
02 activated channels in rat retinal ganglion cells: uncompetitive antagonism. *Journal*
03 *of Physiology-London* **499**, 27–46.
- 04 11. Parsons, C.G., S. Hartmann, and P. Spielmanns (1998) Budipine is a low affinity,
05 N-methyl-D-aspartate receptor antagonist: patch clamp studies in cultured striatal,
06 hippocampal, cortical and superior colliculus neurones. *Neuropharmacology* **37**,
07 719–727.
- 08 12. Parsons, C.G., V.A. Panchenko, V.O. Pinchenko, A.Y. Tsyndrenko, and O.A.
09 Krishtal (1996) Comparative patch-clamp studies with freshly dissociated rat
10 hippocampal and striatal neurons on the NMDA receptor antagonistic effects of
11 amantadine and memantine. *The European Journal of Neuroscience* **8**, 446–454.
- 12 13. Parsons, C.G., G. Quack, I. Bresink, L. Baran, E. Przegalinski, W. Kostowski,
13 P. Krzascik, S. Hartmann, and W. Danysz (1995) Comparison of the potency,
14 kinetics and voltage-dependency of a series of uncompetitive NMDA receptor
15 antagonists in-vitro with anticonvulsive and motor impairment activity in-vivo.
16 *Neuropharmacology* **34**, 1239–1258.
- 17 14. Sobolevsky, A. and S. Koshelev (1998) Two blocking sites of amino-adamantane
18 derivatives in open N-methyl-d-aspartate channels. *Biophysical Journal* **74**,
19 1305–1319.
- 20 15. Sobolevsky, A.I., S.G. Koshelev, and B.I. Khodorov (1998) Interaction of memantine
21 and amantadine with agonist-unbound NMDA-receptor channels in acutely
22 isolated rat hippocampal neurons. *Journal of Physiology-London* **512**, 47–60.
- 23 16. Clark, G.D., D.B. Clifford, and C.F. Zorumski (1990) The effect of agonist
24 concentration, membrane voltage and calcium on N-methyl-D-aspartate receptor
25 desensitization. *Neuroscience* **39**, 787–797.
- 26 17. Grantyn, R. and H.D. Lux (1988) Similarity and mutual exclusion of NMDA-
27 activated and proton-activated transient Na⁺-currents in rat tectal neurons. *Neuro-*
28 *science Letters* **89**, 198–203.
- 29 18. Zilberter, Y., V. Uteshev, S. Sokolova, and B. Khodorov (1991) Desensitization of
30 N-methyl-D-aspartate receptors in neurons dissociated from adult-rat hippocampus.
31 *Molecular Pharmacology* **40**, 337–341.
- 32 19. Johnson, J.W. and P. Ascher (1987) Glycine potentiates the NMDA response in
33 cultured mouse-brain neurons. *Nature* **325**, 529–531.
- 34 20. Parsons, C.G., X.G. Zong, and H.D. Lux (1993) Whole-cell and single-channel
35 analysis of the kinetics of glycine-sensitive N-methyl-D-aspartate receptor desensitization.
36 *British Journal of Pharmacology* **109**, 213–221.
- 37 21. Hashimoto, A. and T. Oka (1997) Free D-aspartate and D-serine in the mammalian
38 brain and periphery. *Progress in Neurobiology* **52**, 325–353.
- 39 22. Hamill, O.P., A. Marty, E. Neher, B. Sakmann, and F.J. Sigworth (1981) Improved
patch-clamp techniques for high resolution current recording from cells and
cell-free membrane patches. *Pflugers Archiv: European Journal of Physiology* **391**,
85–100.

- 01 23. Sigworth, F.J., H. Affolter, and E. Neher (1995) Design of the Epc-9, a computer-
02 controlled patch-clamp amplifier. 2. Software. *Journal of Neuroscience Methods*
03 **56**, 203–215.
- 04 24. Albuquerque, E.X., E.F.R. Pereira, N.G. Castro, M. Alkondon, S. Reinhardt,
05 H. Schroder, and A. Maelicke (1995) Nicotinic receptor function in the mammalian
06 central-nervous-system, in *Diversity of Interacting Receptors*. New York Acad
07 Sciences: New York, pp. 48–72.
- 08 25. Black, M., T. Lanthorn, D. Small, G. Mealing, V. Lam, and P. Morley (1996)
09 Study of potency, kinetics of block and toxicity of NMDA receptor antagonists
10 using fura-2. *European Journal of Pharmacology* **317**, 377–381.
- 11 26. Rogawski, M.A., S.I. Yamaguchi, S.M. Jones, K.C. Rice, A. Thurkauf,
12 and J.A. Monn (1991) Anticonvulsant activity of the low-affinity uncompet-
13 itive N-methyl-D-aspartate antagonist (+/–)-5-aminocarbonyl-10,11-dihydro-5h-
14 dibenzo[a,D]cyclohepten-5, 10-imine (Adci) – comparison with the structural
15 analogs dizocilpine (Mk-801) and carbamazepine. *The Journal of Pharmacology*
16 *and Experimental Therapeutics* **259**, 30–37.
- 17 27. Frankiewicz, T., B. Potier, Z.I. Bashir, G.L. Collingridge, and C.G. Parsons
18 (1996) Effects of memantine and MK-801 on NMDA-induced currents in cultured
19 neurones and on synaptic transmission and LTP in area CA1 of rat hippocampal
20 slices. *British Journal of Pharmacology* **117**, 689–697.
- 21 28. Chen, H.S.V., J.W. Pellegrini, S.K. Aggarwal, S.Z. Lei, S. Warach, F.E. Jensen,
22 and S.A. Lipton (1992) Open-channel block of N-methyl-D-aspartate (NMDA)
23 responses by memantine – therapeutic advantage against NMDA receptor-mediated
24 neurotoxicity. *Journal of Neuroscience* **12**, 4427–4436.
- 25 29. Clements, J.D., R.A.J. Lester, G. Tong, C.E. Jahr, and G.L. Westbrook (1992) The
26 time course of glutamate in the synaptic cleft. *Science* **258**, 1498–1501.
- 27 30. Nowak, L., P. Bregestovski, P. Ascher, A. Herbet, and A. Prochiantz (1984)
28 Magnesium gates glutamate-activated channels in mouse central neurons. *Nature*
29 **307**, 462–465.
- 30 31. Andine, P., M. Sandberg, R. Bagenholm, A. Lehmann, and H. Hagberg (1991)
31 Intracellular and extracellular changes of amino-acids in the cerebral-cortex of
32 the neonatal rat during hypoxic-ischemia. *Brain Research. Developmental Brain*
33 *Research* **64**, 115–120.
- 34 32. Benveniste, H., J. Drejer, A. Schousboe, and N.H. Diemer (1984) Elevation of the
35 extracellular concentrations of glutamate and aspartate in rat hippocampus during
36 transient cerebral-ischemia monitored by intracerebral microdialysis. *Journal of*
37 *Neurochemistry* **43**, 1369–1374.
- 38 33. Buisson, A., J. Callebert, E. Mathieu, M. Plotkine, and R.G. Boulu (1992) Striatal
39 protection induced by lesioning the substantia-nigra of rats subjected to focal
ischemia. *Journal of Neurochemistry* **59**, 1153–1157.
- 34 34. Globus, M.Y.T., R. Busto, E. Martinez, I. Valdes, W.D. Dietrich, and
M.D. Ginsberg (1991) Comparative effect of transient global-ischemia on

- 01 extracellular levels of glutamate, glycine, and gamma-aminobutyric-acid in
02 vulnerable and nonvulnerable brain-regions in the rat. *Journal of Neurochemistry*
03 **57**, 470–478.
- 04 35. Globus, M.Y.T., M.D. Ginsberg, and R. Busto (1991) Excitotoxic index – a
05 biochemical marker of selective vulnerability. *Neuroscience Letters* **127**, 39–42.
- 06 36. Mitani, A., Y. Andou, and K. Kataoka (1992) Selective vulnerability of
07 hippocampal Ca1 neurons cannot be explained in terms of an increase in glutamate
08 concentration during ischemia in the gerbil – brain microdialysis study. *Neuro-*
09 *science* **48**, 307–313.
- 10 37. Sobkowicz, H.M. and S.M. Slapnick (1992) Neuronal sprouting and synapse
11 formation in response to injury in the mouse organ of corti in culture. *International*
12 *Journal of Developmental Neuroscience: The Official Journal of the International*
13 *Society for Developmental Neuroscience* **10**, 545–566.
- 14 38. Sobkowicz, H.M., S.M. Slapnick, and B.K. August (1993) Presynaptic fibers of
15 spiral neurons and reciprocal synapses in the organ of corti in culture. *Journal of*
16 *Neurocytology* **22**, 979–993.
- 17 39. Davies, S.N., D. Martin, J.D. Millar, J.A. Aram, J. Church, and D. Lodge (1988)
18 Differences in results from invivo and invitro studies on the use-dependency of
19 N-methylaspartate antagonism by Mk-801 and other phencyclidine receptor
20 ligands. *European Journal of Pharmacology* **145**, 141–151.
- 21 40. Coan, E.J., A.J. Irving, and G.L. Collingridge (1989) Low-frequency activation of
22 the NMDA receptor system can prevent the induction of Ltp. *Neuroscience Letters*
23 **105**, 205–210.
- 24 41. Frankiewicz, T. and C.G. Parsons (1999) Memantine restores long term poten-
25 tiation impaired by tonic N-methyl-D-aspartate (NMDA) receptor activation
26 following reduction of Mg²⁺ in hippocampal slices. *Neuropharmacology* **38**,
27 1253–1259.
- 28 42. Furukawa, Y., M. Okada, N. Akaike, T. Hayashi, and J. Nabekura (2000) Reduction
29 of voltage-dependent magnesium block of N-methyl-D-aspartate receptor-mediated
30 current by in vivo axonal injury. *Neuroscience* **96**, 385–392.
- 31 43. Rogawski, M.A. and G.L. Wenk (2003) The neuropharmacological basis for the
32 use of memantine in the treatment of Alzheimer’s disease. *CNS Drug Reviews* **9**,
33 275–308.
- 34 44. Wang, L.Y. and J.F. Macdonald (1995) Modulation by magnesium of the affinity
35 of NMDA receptors for glycine in murine hippocampal-neurons. *Journal of*
36 *Physiology-London* **486**, 83–95.
- 37
38
39

01 **QUERIES TO BE ANSWERED (SEE MARGINAL MARKS)**

02 **IMPORTANT NOTE: Please mark your corrections and answers to these**
 03 **queries directly onto the proof at the relevant place. Do NOT mark your**
 04 **corrections on this query sheet.**

06 Chapter-02

08 Query No.	Page No.	Line No.	Query
09 AQ1	16	34	In the sentence 'In addition, the unblocking kinetics are voltage dependent, and this aspect cannot be addressed by using ramping protocols in voltage-dependency experiments (see below)', please be specific about the section number rather than the phrase 'see below'.
17 AQ2	17	Running head	Please check if the running head is OK.
19 AQ3	17	03	In the sentence 'The contribution of voltage-activated calcium channels upon the currents measured can be reduced by lowering Ca ²⁺ in the extracellular solution (see below)', please be specific about the section number rather than the phrase 'see below'.
27 AQ4	17	07	Please clarify whether the text '10s of seconds' means 'tens of seconds' in the sentence 'The contribution of all voltage-activated channels. ...'
31 AQ5	17	12	In the sentence 'However, such protocols are long and are associated with other potential problems (see below)', please be specific about the section number rather than the phrase 'see below'.

Query No.	Page No.	Line No.	Query
AQ6	17	16	In the sentence 'This problem can be minimized by decreasing Ca ²⁺ concentrations in the solutions used (see also above)', please be specific about the section number rather than the phrase 'see also above'.
AQ7	17	36	Please provide the full form of 'ATP'
AQ8	17	36	In the sentence 'Aside from the various forms of receptor desensitization detailed above, NMDA receptors...', please be specific about the section number rather than the phrase 'detailed above'.
AQ9	19	11	Please provide the full form of 'EGTA'.
AQ10	19	13	Please provide the full form of 'cAMP'.
AQ11	19	23	Please provide the full form of 'PCP'.
AQ12	19	29	The text 'Hank's buffered salt solution' has been changed to 'Hanks' buffered salt solution'. Please check if this is OK.
AQ13	21	04	Please clarify if the text '200–250 μM' is OK in the sentence 'The openings of the square-walled'
AQ14	21	39	In the sentence 'The composition of the intracellular solution used when recording NMDA receptor mediated from hippocampal neurons is given in Subheading 2.2.14', please clarify whether the given subheading number is OK as there seems to be no such subheading.
AQ15	22	09	In the sentence 'The corresponding extracellular bath solution composition is given in Subheading 2.2.15', please clarify whether the given subheading number is OK as there seems to be no such subheading.

01	Query No.	Page No.	Line No.	Query
02				
03	AQ16	23	05	In Table 1, please provide the full form
04				of 'PCP' and also clarify whether the
05				deletion of the abbreviation 'NT' is OK
06				as it is not mentioned in the table.
07	AQ17	26	12	In the sentence 'Blockade was expressed
08				as a percentage of the mean control
09				current recorded before and after the
10				application of antagonist, as in the
11				kinetic experiments described above',
12				please be specific about the section
13				number rather than the phrase 'described
14				above'.
15	AQ18	30	14	Please provide the citations for all the
16				notes.
17	AQ19	30	24	Please provide the full form of 'ARL'.
18	AQ20	30	24	Please provide the full form of 'ADCI'.
19	AQ21	30	34	Please provide the full form of 'EPSP'.
20	AQ22	33	16	In 'Reisberg et al., 2003', the end page
21				number '610' has been changed to '612'.
22				Please clarify whether this is OK.
23				
24				
25				
26				
27				
28				
29				
30				
31				
32				
33				
34				
35				
36				
37				
38				
39				